PROTEINS: Structure, Function, and Bioinformatics 54:237–246 (2004)

Free Energies of Binding of Polychlorinated Biphenyls to the Estrogen Receptor From a Single Simulation

Chris Oostenbrink and Wilfred F. van Gunsteren*
Laboratory of Physical Chemistry, Swiss Federal Institute of Technology Zürich, Zürich, Switzerland

ABSTRACT **Relative free energies of binding to the ligand-binding domain of the estrogen receptor have been calculated for a series of 17 hydroxylated polychlorinated biphenyls. Because traditional thermodynamic integration or perturbation approaches are hardly feasible for these numbers of compounds, the one-step perturbation approach is applied and is shown to yield accurate results based on only two 2-ns molecular dynamics simulations of an unphysical, judiciously chosen, reference state. The mean absolute difference between the calculated and experimental binding free energies for the 17 compounds is 3.4 kJ/mol, which illustrates the accuracy of the GROMOS biomolecular force field used. Excluding the three largest ligands from the comparison reduces the deviation to 2.0 kJ/mol (i.e., $< k_B T$). Apart from the relative free energy, structural information about the binding mode and binding orientation for every compound can also be extracted from the simulation, showing that a ligand bound to its receptor cannot be represented by a single conformation, but it samples an ensemble of different orientations. Proteins 2004;54:237–246.**

Key words: molecular dynamics simulation; single-step perturbation; soft-core interaction; binding modes

INTRODUCTION

The prediction of binding affinities for series of compounds remains one of the major challenges for computational chemistry. Empirical methods often require large amounts of data to be available beforehand, whereas a parameter-free approach is usually too computationally demanding to be applied to more than a handful of compounds. However, it has been proposed that by using a judiciously chosen unphysical reference state, the computation of a relative free energy can be made orders of magnitude more efficient at the expense of a slight loss in accuracy.[1] We have calculated relative free energies of binding for a series of 17 hydroxylated polychlorinated biphenyls (PCBs) to the ligand-binding domain (LBD) of the estrogen alpha receptor (ERα). The calculations were based on two 2-ns molecular dynamics simulations and the perturbation formula, keeping the computational costs low.

The estrogen receptor plays a key role in the growth, development, and maintenance of a diverse range of tissues. The activity of the estrogen receptor is triggered by the binding of an estrogen to the LBD, allowing for the translocation of the receptor protein to the nucleus, where the DNA-binding domain of the receptor interacts directly with response elements on the DNA, activating or repressing transcription.[2] Naturally occurring estrogens are steroid hormones, such as the endogenous ligand, 17β-estradiol. Apart from this endogenous ligand, the estrogen receptor is known to show affinity for a wide range of structurally diverse compounds, including synthetic estrogens, polyaromatic hydrocarbons, phytoestrogens, pesticides, and polychlorinated biphenyls.[3–7]

Although the production and use of polychlorinated biphenyls was banned in the late 1970s, they have still been observed in all kinds of tissues and species.[8–10] One of the metabolic pathways of the PCBs involves the hydroxylation of (one of the) aromatic rings,[11] after which the affinity for the estrogen receptor is altered.[12] It is reasonable to suspect that this hydroxyl group takes over the function of the aromatic hydroxyl group in the endogenous ligand. Among other pathways [e.g., involving the aryl hydrocarbon (Ah) receptor signaling pathway], the PCBs are known to disrupt the endocrine system by a direct action on the estrogen receptor.[13–15]

In the present study, we have calculated the relative binding free energies for a group of 17 hydroxylated PCBs, shown in Figure 1. The experimental values listed in Figure 1 have been taken from the literature as a reference to assess the accuracy of our calculations. The hydroxyl group was always assumed to be oriented comparably to the estradiol aromatic hydroxyl group, allowing the formation of hydrogen bonds with Glu 353 and Arg 394 and an internal water molecule.[16–18] Other compounds that show a high affinity for the estrogen receptor often contain a second hydroxyl group at approximately 1.1 nm from the first.[19] This hydroxyl group is known to form hydrogen bonds to residue His 524.[16–18]

*Correspondence to: Wilfred F. van Gunsteren, Laboratory of Physical Chemistry, Swiss Federal Institute of Technology Zürich, ETH-Hönggerberg, 8093 Zürich, Switzerland. E-mail: wfvgn@igc.phys.chem.ethz.ch

Received 16 April 2003; Accepted 12 June 2003

Code	$\Delta\Delta G^{bind}_{exp}$	#
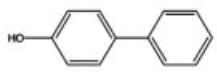 0CBOH1 4-biphenylol	23.0[a]	1
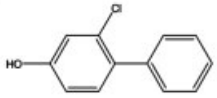 1CBOH1 2-chlorobiphenyl-4-ol	19.5[a] 17.8[b]	2
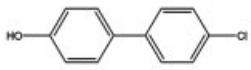 1CBOH2 4'-chlorobiphenyl-4-ol	20.6[a] 19.1[b]	1
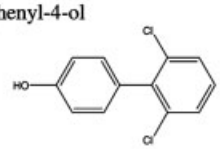 2CBOH1 2',6'-dichlorobiphenyl-4-ol	14.9[a] 11.9[b]	1
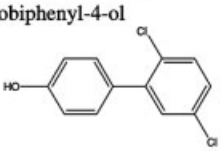 2CBOH2 2',5'-dichloro-biphenyl-4-ol	15.5[a] 12.3[b] 19.8[c]	2
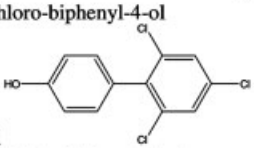 3CBOH1 2',4',6'-trichlorobiphenyl-4-ol	6.9[d] 7.3[b] 9.4[a]	1
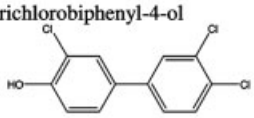 3CBOH2 3,3',4'-trichlorobiphenyl-4-ol	14.5[d]	4
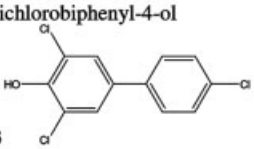 3CBOH3 3,4',5-trichlorobiphenyl-4-ol	17.2[a]	1
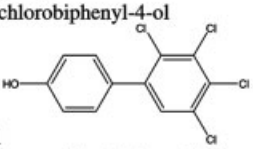 4CBOH1 2',3',4',5'-tetrachlorobiphenyl-4-ol	8.5[d] 9.3[e] 7.1[b] 11.4[a]	2

Code	$\Delta\Delta G^{bind}_{exp}$	#
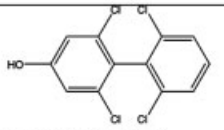 4CBOH2 2,2',6,6'-tetrachlorobiphenyl-4-ol	15.3[c] 13.3[e]	1
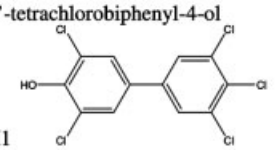 5CBOH1 3,3',4',5,5'-pentachlorobiphenyl-4-ol	21.2[d]	1
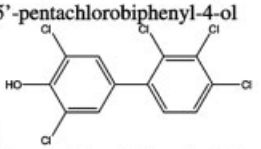 5CBOH2 2',3,3',4',5-pentachlorobiphenyl-4-ol	17.2[d]	2
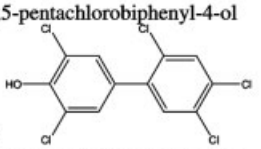 5CBOH3 2',3,4',5,5'-pentachlorobiphenyl-4-ol	12.0[d]	2
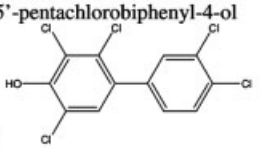 5CBOH4 2,3,3',4',5-pentachlorobiphenyl-4-ol	11.5[d]	4
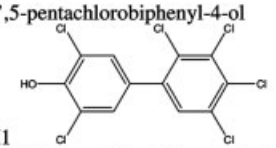 6CBOH1 2',3,3',4',5,5'-hexachlorobiphenyl-4-ol	8.6[d]	2
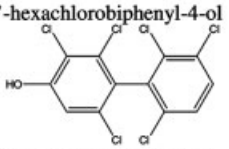 6CBOH2 2,2',3,3',6,6'-hexachlorobiphenyl-4-ol	19.7[b]	4
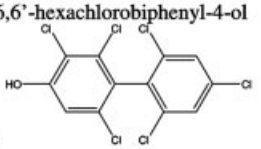 6CBOH3 2,2',3,4',6,6'-hexachlorobiphenyl-4-ol	16.0[b]	2
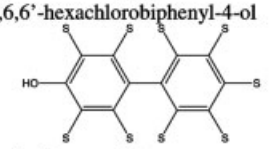 REF Unphysical reference state		

Fig. 1. Molecular structures of the hydroxylated polychlorinated biphenyls. Experimental free energies of binding ($\Delta\Delta G^{bind}_{exp}$) in kJ/mol, relative to 17β-estradiol. The next column, symbol # indicates the number of different binding modes due to the distribution of the chlorine atoms over the rings. Experimental data taken from the following: **a:** Ref. 41; **b:** Ref. 6; **c:** Ref. 42; **d:** Ref. 43; and **e:** Ref. 12. The reference ligand REF contains soft atoms (S) at sites that can be chlorinated.

Quantitative structure activity relationship (QSAR) studies indicate that the proximal hydroxyl (interacting with residues Glu 353 and Arg 394) is required for binding, whereas the distal hydroxyl (interacting with His 524) contributes only weakly to binding and is suggested to serve merely as a means to improve the solubility of the native hormone.[19] Depending on the distribution of the chlorine atoms over the molecule, one, two, or four possible binding modes remain, assuming that the two aromatic rings are approximately perpendicular to each other. The number of binding modes that were considered for every compound is also listed in Figure 1.

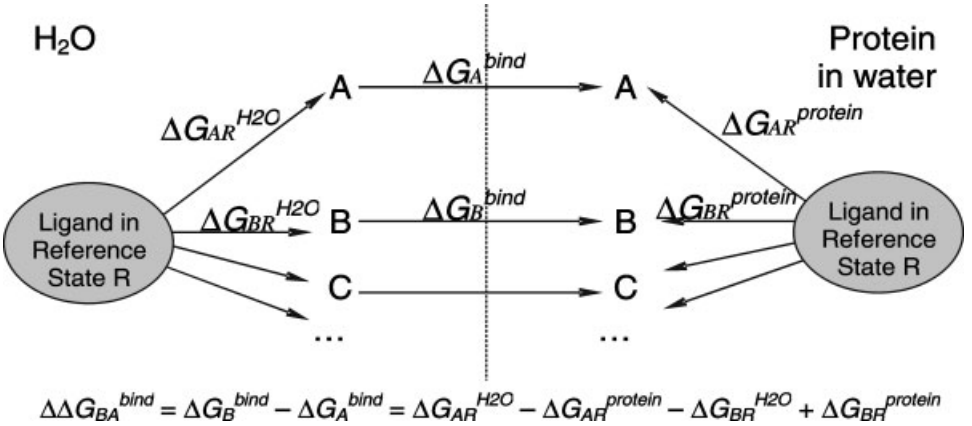

Fig. 2. Thermodynamic scheme used to calculate relative free energies ΔG of binding for compounds A, B, … from two simulations of the reference ligand indicated by R.

MATERIALS AND METHODS

The free energy difference between a reference state (R) and another state (A) can be calculated from a simulation of state R using the perturbation formula

$$\Delta G_{\mathrm{AR}} = -\mathrm{k_B}T\ln\langle e^{-(E_\mathrm{A}-E_\mathrm{R})/\mathrm{k_B}T}\rangle_\mathrm{R} \qquad (1)$$

where E_R and E_A represent the potential energies of the system in states R and A, respectively, $\mathrm{k_B}$ is the Boltzmann constant, T is the temperature, and the brackets indicate an ensemble average from the simulation of state R.[20] For drug design purposes, states R and A would typically represent different ligands bound to a protein. However, in the case of finite sampling, Eq. 1 will only give a reasonable estimate if the ensemble generated for state (ligand) R shows considerable overlap with an ensemble that would be generated for state (ligand) A. For physically meaningful applications, this will hardly ever be the case.

In the standard free energy perturbation (FEP) approach or when using the thermodynamic integration (TI) approach, this problem is usually tackled by dividing the change from R to A into a number of small changes or steps, and calculating the free energy between them as the sum of the free energy differences between these steps. A sufficiently long simulation at each of these steps is then required, from which one can apply Eq. 1 to get an estimate of the free energy difference toward the next step.[20–22] The large computational effort that is needed makes the standard application of FEP or TI for drug design purposes practically unfeasible, especially if the relative binding free energies of a series of compounds needs to be estimated.

Our approach has rather been to design an (unphysical) reference state R for which we can generate an ensemble which is broad enough to show overlap with ensembles of several real ligands A, B, etc.[1,23] From this ensemble, we can directly apply Eq. 1 and get an estimate of the free energy change between the reference state and these real ligands in one single step.[24–26] This calculation can be applied to the trajectories of two molecular dynamics (MD) simulations, one of the unphysical reference ligand R in water and one where R is bound to the receptor. Postprocessing of the MD trajectories, applying Eq. 1 allows us to calculate the relative free energies of binding for all real compounds, as is depicted in Figure 2.

The ligand reference state that was used in the calculation of relative free energies of binding for the hydroxyl-PCBs in this study is shown in the lower right corner of Figure 1 and is labeled REF. In this compound, the atoms designated with S are so-called soft atoms (i.e., their nonbonded interaction function has been modified to remove the singularity at the origin). This has the effect that other atoms can occasionally show overlap with the soft atoms. In practice, this is achieved by writing the Lennard–Jones interaction for the atoms i and j with Cartesian coordinates $\mathbf{r_i}$ and $\mathbf{r_j}$ as[1,27]:

$$E^{\mathrm{vdw}}(\mathbf{r_{ij}}) = \left(\frac{C12}{\alpha + \mathbf{r}_{\mathbf{ij}}^6} - C6\right)\frac{1}{\alpha + \mathbf{r}_{\mathbf{ij}}^6} \qquad (2)$$

where α is a small offset to the distance between the atoms, $r_{ij} \equiv |\mathbf{r_{ij}}| \equiv |\mathbf{r_i} - \mathbf{r_j}|$ and $C6$ and $C12$ are the van der Waals interaction parameters of the force field for the particular pair of atoms.

Figure 3 shows the effect of this modification: the interaction energy (Eq. 2) between a carbon atom and an atom X has been plotted as a function of the interatomic distance for different types of X. The solid curve corresponds to the case where X is a real chlorine atom; the dotted curve corresponds to X being a real hydrogen atom. The dashed curve shows the effect of softening the chlorine atom. The dash-dot and dash-dash-dot curves are included to show that nonsoft repulsion by the carbon atom CX to which atom X is bound will prevent the approaching carbon atom from completely overlapping with atom X.

For the real ligands (A, B, … in Fig. 2) we have used the hydroxylated PCBs of Figure 1 in all different binding modes. In an isotropic medium such as water, the different binding modes should be indistinguishable and yield the

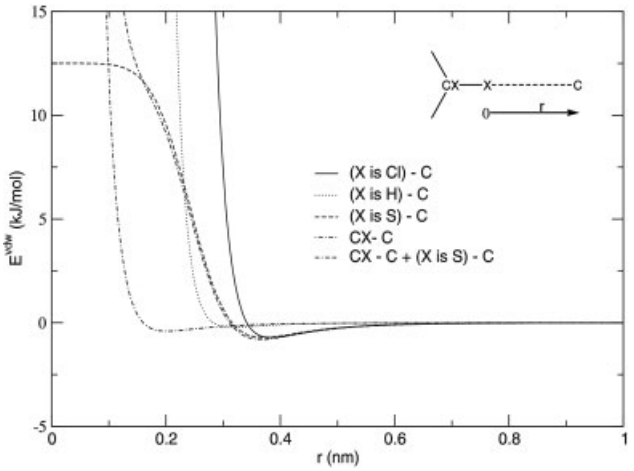

Fig. 3. Comparison of van der Waals interaction for a carbon atom (C) approaching atom X that is bound to carbon atom CX at a distance of 0.1758 nm as a function of *r*. X is a real chlorine atom (solid); X is a real hydrogen atom (dotted); X is an unphysical, soft chlorine atom with $\alpha = 0.3775 \times C12/C6$ (dashed). Interaction between the approaching carbon (C) and the carbon atom (CX) to which X is bound (dash-dot). Sum of dash and dash-dot curves (dash-dash-dot).

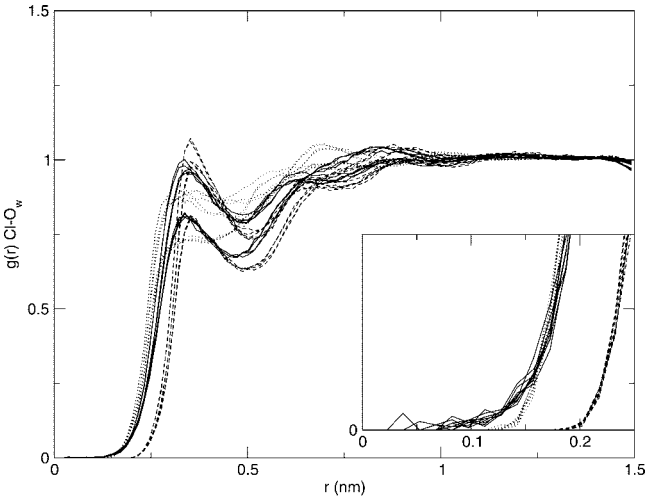

Fig. 4. Radial distribution functions of water (oxygen atoms) surrounding nine X atoms in the reference ligand (see Fig. 1). X are real chlorine atoms (dashed), X are real hydrogen atoms (dotted), X are soft chlorine atoms (solid).

same free energies for a given compound. In an anisotropic environment, this will not be the case, and the differences in free energy between binding modes will allow us to identify preferred binding modes for the individual compounds from the simulation.

RESULTS

Two 2-ns-long MD simulations were conducted, one of the unphysical reference ligand REF in water and one where REF was bound to the ligand-binding domain of the ERα in water. After insertion of the reference ligand, the atom positional root-mean-square deviation (RMSD) from the X-ray crystal structure for the protein backbone atoms stayed around a value of ~0.12 nm, indicating that the protein remained stable. During the simulation, the reference ligand remains hydrogen bonded to Glu 353 for 90% of the time.

The effect of softening the atoms can be observed in Figure 4, where the radial distribution functions of the soft atoms with water oxygen atoms from the water simulation (solid curves) is compared with the same radial distribution functions evaluated from 1-ns simulations of the reference ligand with real chlorine atoms (dashed curves) and real hydrogen atoms (dotted curves) at all nine soft sites. It is clear that when interacting with soft atoms, the water molecules are allowed to overlap with the soft sites, whereas at longer distances they behave as if interacting with chlorine atoms.

Table I lists the results of the one-step perturbation calculations. For numerical reasons, the replacement of the reference compound R by a real compound A was considered as a two-step process:

$$\text{ER:R} \rightarrow \text{ER:(R:A)*} \rightarrow \text{ER:A} \qquad (3)$$

First, the real compound A was added to the reference compound-protein complex, forming an ER:(R:A)* complex, where the symbol * indicates the omission of the interaction between compounds R and A. The energy of this complex is

$$E_{\text{ER:(R:A)*}} = E_{\text{ER,ER}} + E_{\text{ER,R}} + E_{\text{R,R}} + E_{\text{ER,A}} + E_{\text{A,A}} \qquad (3A)$$

and the energy of the ER:R complex is

$$E_{\text{ER:R}} = E_{\text{ER,ER}} + E_{\text{ER,R}} + E_{\text{R,R}} \qquad (3B)$$

the interaction between two parts A and B of a system being indicated by $E_{\text{A,B}}$. The free energy for the first step of process (Eq. 3) can be calculated by using Eq. 1 as

$$G_{\text{ER:(R:A)*}} - G_{\text{ER:R}} = -k_B T \ln\langle e^{-(E_{\text{ER,A}} + E_{\text{A,A}})/k_B T}\rangle_{\text{ER:R}} \qquad (4)$$

The second step involves the removal of R from this complex. We assume that this free energy is identical for each real compound A considered here. In other words, it is assumed that the interaction energy between the protein and the reference compound R will only slightly be influenced by the differences between the real compounds A.

For the compounds that allow the probing of several binding orientations, the results for the individual orientations appear in Table I marked with a, b, … The combined results have been obtained by including all orientations in the ensemble average of Eq. 1. For any pair of compounds, the difference between the values listed in the column marked $\Delta\Delta G_{XR}^{bind}$ of Table I yields the relative free energy of binding and can be compared to the difference in experimental binding free energies. Because the absolute free energies are unknown, only relative free energies can be compared. Rather than selecting one compound as a reference, we compare our results by shifting all calculated $\Delta\Delta G_{XR}^{bind}$ by a value of

TABLE I. Various Free Energies (in kJ/mol) Obtained by One-Step Perturbation Calculations and Experiment for a Series of Hydroxylated Polychlorinated Biphenyls[†]

	Computed from two simulations				Experimental
Compound	$\Delta G_{XR}^{H_2O}$	$\Delta G_{XR}^{protein}$	$\Delta\Delta G_{XR}^{bind}$	$\Delta\Delta G_{calc}^{bind,\ shifted}$	$\Delta\Delta G_{exp}^{bind}$
0CBOH1	−102.5	−126.3	−23.8	23.7	23.0[a]
1CBOH1 *a*	−84.7	−109.7	−25.0	22.5	
b	−85.0	−113.5	−28.5	19.0	
comb	−84.9	−112.3	−27.4	21.1	19.5[a]
1CBOH2	−112.8	−143.4	−30.6	16.9	20.6[a]
2CBOH1	−108.5	−138.2	−29.7	17.8	14.9[a]
2CBOH2 *a*	−119.6	−152.4	−32.8	14.7	
b	−121.2	−150.6	−29.4	18.1	
comb	−120.5	−151.6	−31.1	16.4	15.5[a]
3CBOH1	−112.3	−147.9	−35.6	11.9	6.9[d]
3CBOH2 *a*	−113.2	−148.1	−34.9	12.6	
b	−113.6	−151.4	−37.8	9.7	
c	−113.6	−143.6	−30.0	17.5	
d	−114.6	−143.2	−28.6	18.9	
comb	−113.8	−148.7	−34.9	12.6	14.5[d]
3CBOH3	−105.3	−136.2	−30.9	16.6	17.2[a]
4CBOH1 *a*	−124.0	−168.1	−44.1	3.4	
b	−124.5	−157.6	−33.1	14.4	
comb	−124.3	−166.4	−42.1	5.3	8.5[d]
4CBOH2	−69.4	−100.4	−31.0	16.5	15.3[c]
5CBOH1	−104.6	−131.3	−26.7	20.8	21.2[d]
5CBOH2 *a*	−108.4	−136.6	−28.2	19.3	
b	−105.7	−143.8	−38.1	9.4	
comb	−107.4	−142.2	−34.8	12.7	17.2[d]
5CBOH3 *a*	−122.6	−156.6	−34.0	13.5	
b	−115.5	−147.2	−31.7	15.8	
comb	−121.0	−155.0	−34.0	13.5	12.0[d]
5CBOH4 *a*	−107.5	−126.0	−18.5	29.0	
b	−98.1	−135.7	−37.6	9.9	
c	−103.7	−142.7	−39.0	8.4	
d	−98.6	−135.5	−36.9	10.6	
comb	−104.6	−139.6	−35.0	12.5	11.5[d]
6CBOH1 *a*	−125.7	−150.3	−24.6	22.9	
b	−119.4	−147.6	−28.2	19.3	
comb	−124.2	−149.3	−25.1	22.4	8.6[d]
6CBOH2 *a*	−101.0	−122.6	−21.6	25.9	
b	−89.1	−120.4	−31.3	16.2	
c	−89.2	−126.1	−36.9	10.6	
d	−94.7	−118.6	−23.9	23.6	
comb	−97.8	−123.5	−25.7	21.8	19.7[b]
6CBOH3 *a*	−75.7	−123.3	−47.7	−0.2	
b	−75.2	−116.6	−41.4	6.1	
comb	−75.5	−121.7	−46.2	1.3	16.0[b]

[†]The ligands are defined in Figure 1, and the different free energies in Figure 2. If ligands have more than one binding orientation, these are indicated by the symbols *a–d*. The symbol *comb* indicates the free energy as obtained by averaging over all binding orientations. Experimental data were taken from the following:
[a]Ref. 41.
[b]Ref. 6.
[c]Ref. 42.
[d]Ref. 43.
[e]Ref. 12.

47.5 kJ/mol, resulting in $\Delta\Delta G_{calc}^{bind,shifted}$, leading to the optimum fit to the experimental values $\Delta\Delta G_{exp}^{bind}$ (which are relative to the endogenous ligand, 17β-estradiol). The last two columns of Table I have been plotted in Figure 5. The straight diagonal line corresponds to an exact reproduction of the experimental results. The horizontal lines connect different experimental values that have been reported in the literature for the same compound (see Fig. 1).

DISCUSSION

Figure 6 shows the development of $\Delta G_{XR}^{protein}$ as a function of time in case the real ligand X is 5CBOH3, in orientation b. This curve shows the typical one-step saw-

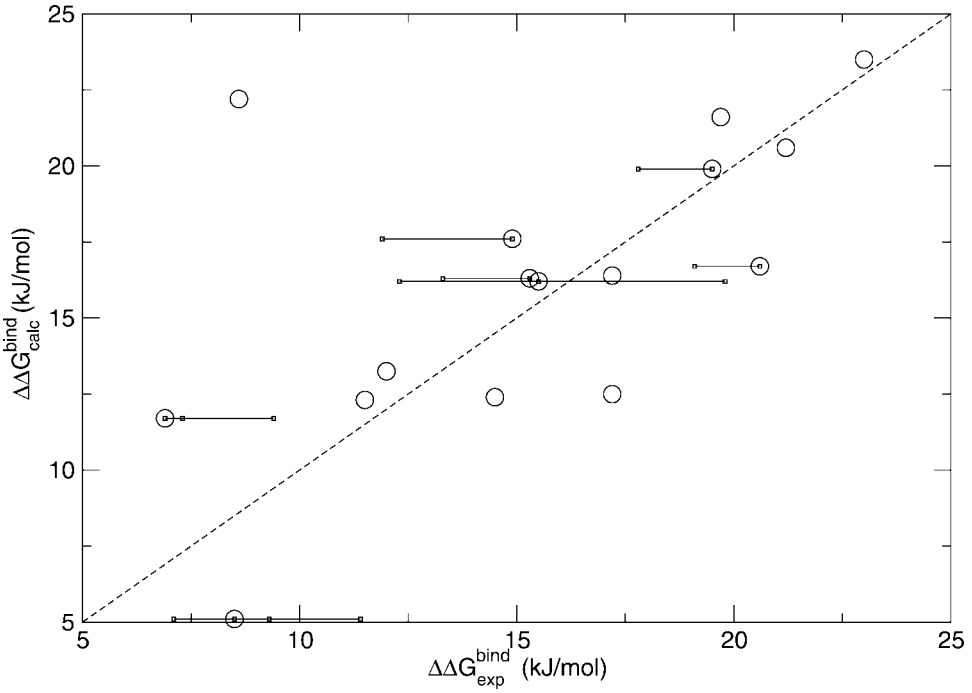

Fig. 5. Experimental versus calculated relative free energies of binding for the 17 hydroxylated biphenyls. The straight diagonal line corresponds to a perfect reproduction of experimental values. Horizontal lines connect different experimental values for one compound. The result for 6CBOH3 is not displayed because it falls off the scale.

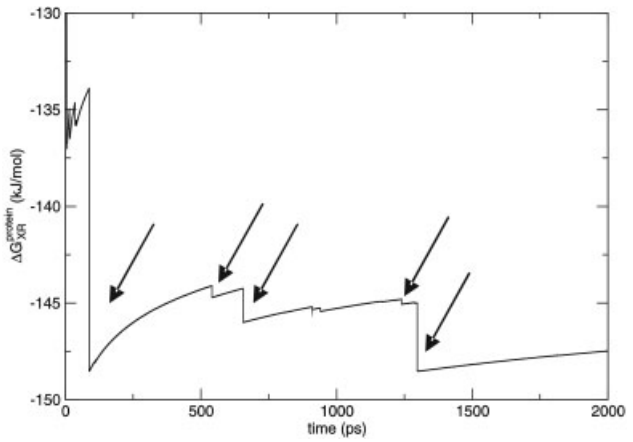

Fig. 6. Development of $\Delta G^{protein}_{XR}$ for compound X is 5CBOH3, orientation b. Arrows indicate the five most contributing (non-neighboring) configurations for this compound, leading to a sharp drop in the free energy estimate as a function of time.

tooth behavior: whenever a conformation of the trajectory that has a favorable energy for this compound is encountered, this conformation will contribute significantly to the ensemble average in Eq. 1 and a corresponding drop in the free energy estimate is observed. As can be seen from this figure, relatively large jumps in the free energy estimate can occur at advanced points in the simulation (e.g., 3.2 kJ/mol at t = 1297.6 ps), making it hard to assess whether the calculation has converged or not. For the compounds that allow for different binding orientations, the water simulations offer a possibility to test convergence. In the ideal case, the different binding orientations should yield the same free energy change in an isotropic medium ($\Delta G^{H_2O}_{XR}$). From Table I, we can see that this is true for compounds containing four or less chlorine atoms but not always for compounds containing more chlorine atoms, with differences of up to 11.9 kJ/mol between orientations for 6CBOH2. The dihedral angle between the two aromatic rings has a mean value of 90.0° ± 20° in the water simulation. A higher number of chlorine atoms reduces the chance of finding similarly favorable configurations, accommodating all chlorine atoms, in calculations for two different orientations.

An asset of the one-step perturbation approach is that for every compound one can identify the configurations that contribute most to its free energy estimate. Figure 7 shows the orientation of the reference state in the five most contributing configurations (see arrows in Fig. 6) in the calculation of $\Delta G^{protein}_{XR}$ (X is 5CBOH3b). This example shows that there is more than a single relevant binding orientation for this compound. The real compound would sample separated areas in configurational space. The secondary ring of the ligand resides between helices 3 and 8 for most of the relevant configurations for this compound but different configurations in which this ring points toward helix 11 are also sampled (around t = 88 ps). Even for the configurations that have the same general orientation of the aromatic rings, the chlorine atoms show displacements of up to 0.23 nm. This finding illustrates that to get a reasonable estimate for the free energy change, one has

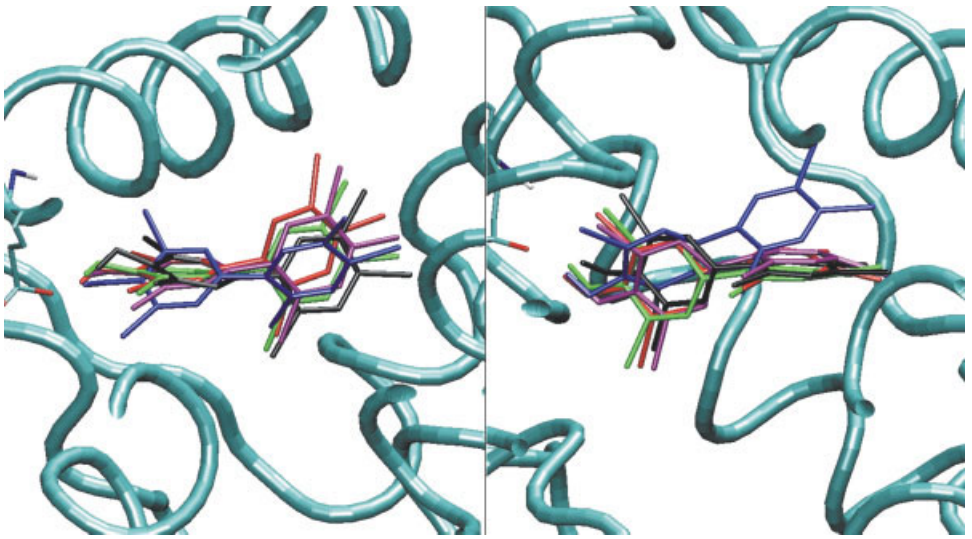

Fig. 7. Superposition of the five orientations of the reference ligand that contribute most to the value of $\Delta G_{XR}^{protein}$ for X is 5CBOH3, orientation b. Configurations correspond to time points indicated by the arrows in Figure 6. **Left:** Top view. **Right:** Side view. To the far left in both panels residue Glu 353 can be seen to form a hydrogen bond with the hydroxyl group of the reference ligand.

to consider the different configurations accessible to the ligand and cannot base an estimate on a single minimum-energy configuration. In addition, a comparison of the binding free energies of different binding modes for one ligand shows that in many cases several binding modes contribute to the overall binding free energy. For example, for 3CBOH2 one can see that the binding modes labeled c and d are contributing equally to the total binding free energy, with a free energy difference between them of less than $k_B T$ (2.5 kJ/mol). On the other hand, the orientations labeled a and b are less likely to be observed. For this compound, modes c and d differ in the position of the chlorine atoms on the nonhydroxylated aromatic ring, as do modes a and b. Modes a and c (b and d) differ in the chlorine position on the hydroxylated ring.

As becomes clear from Figure 1, the experimental values that can be obtained from the literature easily differ several kJ/mol. For inclusion in Table I, we have selected from Figure 1 one experimental value per compound so that the total number of experimental studies from which the selected data have been taken is minimal. Comparing the calculated data to these experimental values yields a mean absolute error of 3.4 kJ/mol. The largest deviations are seen for the compounds with the highest number of chlorine atoms: an overestimation of 13.8 kJ/mol and an underestimation of 14.7 kJ/mol for compounds 6CBOH1 and 6CBOH3, respectively. It is likely that 2 ns of simulation have not been sufficient to sample (enough) conformations that can accommodate six chlorine atoms at the same time. Omitting the hexachlorinated compounds from the analysis yields a mean absolute error of 2.0 kJ/mol for the remaining 14 compounds.

Even a mean absolute error of 3.4 kJ/mol is very satisfactory in view of the experimental uncertainties and compared with results of other methods aimed at estimating free energy differences. The Molecular Mechanics-Poisson–Boltzmann Solvent Accessible surface (MM-PBSA) method, which uses an MD-based, continuum solvent approach typically shows a mean absolute error of 1 kcal/mol (4.2 kJ/mol).[28,29] The Linear Interaction Energy method developed by Aqvist,[30] generally does a bit better with a mean absolute error of 2.5–3 kJ/mol,[31,32] where the parameters used in the LIE equation need to be adapted to the specific system of interest.[33] Both these methods require the simulation of every ligand complexed to the protein for several hundred picoseconds, whereas our results are calculated from two single 2-ns simulations of the reference ligand state, one bound and one unbound to the protein. Moreover, no empirical parameters (other than the ones from the force field) are required to calculate the relative free energies of binding.

Because the actual calculation of free energies is done by postprocessing the previously stored MD trajectories, additional compounds can be added to the series without increasing the overall computational costs significantly as long as the atomic differences between the ligands can be properly represented by using the soft atoms in the reference ligand. To calculate the relative free energy for any additional compound, only the interactions of the ligand atoms with their surroundings need to be computed, because all other interactions remain the same for all compounds. These features make the one-step perturbation approach orders of magnitude more efficient than the standard FEP or TI approaches.

CONCLUSIONS

Relative free energies of binding have been calculated for a series of 17 hydroxylated PCBs, complexed to the ligand-binding domain of the ERα. Only two simulations were required to estimate the relative binding free energies for the whole series. A mean absolute error of 3.4 kJ/mol compared to experimental values indicates a reason-

TABLE II. Nonstandard Force Field Parameters for the Real and Unphysical Ligands Studied.†

Atoms	q (*e*)	Type	$C6^{1/2}$ $(kJ/mol\ nm^6)^{1/2}$	$C12^{1/2}$ $(kJ/mol\ nm^{12})^{1/2}$
H	0.398	18	0.0	0.0
O	−0.548	3	0.04756	$1.125\ 10^{-3}$
C	0.0/0.150[b]	11	0.04838	$1.837\ 10^{-3}$
S[a]	0.0	30	0.09362	$3.911\ 10^{-3}$
HA	0.100[c]	17	0.0092	$0.123\ 10^{-3}$
CI	−0.087[c]	30	0.09362	$3.911\ 10^{-3}$

Bonds	Type	K_b $(kJ\ mol^{-1}\ nm^{-4})$	b_0 (nm)
H–O	1	$15.7\ 10^6$	0.100
O–C	12	$10.2\ 10^6$	0.136
C–C (aromatic)	15	$10.8\ 10^6$	0.139
C–C (connecting rings)	26	$7.15\ 10^6$	0.153
C–S, C–CI	37	$8.12\ 10^6$	0.1758
C–H	3	$12.3\ 10^6$	0.109

Bond angles	Type	K_θ $(kJ\ mol^{-1})$	θ_0 (degree)
H–O–C	11	450.0	109.5
O–C–C, C–C–C, C–C–S, C–C–Cl, C–C–H	26	560.0	120.0

Improper dihedral angles	Type	K_ξ $(kJ\ mol^{-1}\ deg^{-2})$	ξ_0 (degree)
12 per ring	1	0.0510	0.0

Torsional dihedral angles	Type	K_ϕ $(kJ\ mol^{-1})$	cos(δ)	m
H–O–C–C	2	7.11	−1.0	2
C–C–C–C (connecting rings)	1	5.86	−1.0	2

†A soft-core atom is indicated by the symbol S. For definitions of the parameters, see Ref 34.
[a]Soft van der Waals interaction, as in Equation 2, with $\alpha = 0.3775 \times C12/C6$.
[b]The carbon bound to the oxygen has a charge of 0.15 *e*.
[c]In the case of real ligands, the carbon bound to a hydrogen HA, or a chlorine Cl has a charge of −0.100 *e* and 0.087 *e,* respectively.

able accuracy, especially in light of the experimental uncertainties.

Although only two simulations were performed, information on the structural binding modes for all compounds could be obtained, including a structural characterization of the relevant conformations for every compound in a specific binding orientation. Advantages of the one-step perturbation method over other relatively fast methods to calculate free energies are the parameter-free approach and an easy expansion of the series to more hydroxylated PCBs at virtually no additional computational costs.

In conclusion, we have shown that the single-step perturbation approach is a powerful tool for the calculation of relative free energies of binding for a series of compounds. For drug design purposes and for an in silico assessment of the toxic effects of xenochemicals to biological systems, such calculations can be used to predict and possibly replace in vitro or in vivo experiments.

Computational Details

Both simulations were conducted by using the GROMOS96 biomolecular simulation package.[34,35] The parameters for the reference state and the real ligands (see Fig. 1) have been chosen on the basis of similar building blocks of the GROMOS force field, parameter set 43a1, and are summarized in Table II. The value for α in Eq. 2 for the soft atomic interactions was set to $0.3775 \times C12/C6$, the same value that was used in earlier work.[23,25] For the simulation of the reference ligand in water, the molecule was placed in a periodic rectangular box, containing 1228 simple point charge (SPC) water molecules.[36] Initial velocities were randomly assigned according to a Maxwell–Boltzmann distribution at 50 K, after which the system was gradually heated up to a temperature of 300 K increasing the temperature every 5 ps. After 40 ps of equilibration, a 2-ns simulation was performed from which the free energies were calculated.

The starting structure for the protein simulation was taken from a well-equilibrated simulation of the ERα ligand binding domain.[25] The reference ligand was docked into the binding cavity manually by fitting the hydroxylated aromatic ring into the pocket that is occupied by the A-ring of the endogenous ligand.[16,17] The protein was centered in a periodic rectangular box (7.7 × 7.8 × 8.7

nm^3) containing 15824 SPC water molecules[36] and 6 Na^+ ions to obtain a net charge of zero. After adding the reference ligand to the protein, new velocities were assigned to the protein according to a Maxwell–Boltzmann distribution corresponding to a temperature of 300 K and the system was equilibrated for 40 ps before the 2-ns production simulation was started.

Both simulations were conducted at constant temperature and pressure by using the Berendsen algorithm to keep both the temperature and the pressure constant.[37] The water and solute molecules were separately coupled to the temperature bath at 300 K, using a relaxation time (τ_T) of 0.1 ps. The relaxation time for the anisotropic pressure scaling (τ_p) was set to 0.5 ps, with an estimated value of 45.75×10^{-5} (kJ mol^{-1} $nm^{-3})^{-1}$ for the isothermal compressibility[35] and a reference pressure of 1 atm.

Bond lengths were constrained to ideal values by using the SHAKE algorithm,[38] allowing for a timestep of 2 fs. Nonbonded interactions were calculated according to a triple-range cutoff scheme. Interactions within 0.8 nm were calculated every timestep, from a pair list that was generated every fifth timestep. Longer ranged interactions (up to 1.4 nm) were evaluated every fifth timestep as well and kept constant between updates. A reaction field force term[39] was used to approximate electrostatic interactions outside the outer 1.4-nm cutoff, with an effective dielectric constant of 54.0.[40]

Coordinates were stored every 0.1 ps from which the free energies for all compounds and binding modes were later calculated by using a modified version of the program PROFEE in the GROMOS96 package.[35]

REFERENCES

1. Liu HY, Mark AE, van Gunsteren WF. Estimating the relative free energy of different molecular states with respect to a single reference state. J Phys Chem 1996;100:9485–9494.
2. Parker MG, Arbuckle N, Dauvois S, Danielian P, White R. Structure and function of the estrogen-receptor. Ann NY Acad Sci 1993;684:119–126.
3. Blair RM, Fang H, Branham WS, Hass BS, Dial SL, Moland CL, Tong WD, Shi LM, Perkins R, Sheehan DM. The estrogen receptor relative binding affinities of 188 natural and xenochemicals: structural diversity of ligands. Toxicol Sci 2000;54:138–153.
4. Garner CE, Jefferson WN, Burka LT, Matthews HB, Newbold RR. In vitro estrogenicity of the catechol metabolites of selected polychlorinated biphenyls. Toxicol Appl Pharmacol 1999;154:188–197.
5. Breinholt V, Larsen JC. Detection of weak estrogenic flavonoids using a recombinant yeast strain and a modified MCF7 cell proliferation assay. Chem Res Toxicol 1998;11:622–629.
6. Waller CL, Oprea TI, Chae K, Park HK, Korach KS, Laws SC, Wiese TE, Kelce WR, Gray LE. Ligand-based identification of environmental estrogens. Chem Res Toxicol 1996;9:1240–1248.
7. Soto AM, Sonnenschein C, Chung KL, Fernandez MF, Olea N, Serrano FO. The E-screen assay as a tool to identify estrogens—an update on estrogenic environmental-pollutants. Environ Health Perspect 1995;103:113–122.
8. Bergman A, Klassonwehler E, Kuroki H. Selective retention of hydroxylated PCB metabolites in blood. Environ Health Perspect 1994;102:464–469.
9. Jansson B, Andersson R, Asplund L, Litzen K, Nylund K, Sellstrom U, Uvemo UB, Wahlberg C, Wideqvist U, Odsjo T, Olsson M. Chlorinated and brominated persistent organic—compounds in biological samples from the environment. Environ Toxicol Chem 1993;12:1163–1174.
10. Dewailly E, Nantel A, Weber JP, Meyer F. High-levels of PCBs in breast-milk of Inuit women from Arctic Quebec. Bull Environ Contam Toxicol 1989;43:641–646.
11. Sipes IG, Schnellmann RG. Biotransformation of PCBs: metabolic pathways and mechanisms. In: Safe S, editor. Polychlorinated biphenyls (PCBs): mammalian and environmental toxicology. Heidelberg: Springer-Verlag; 1987. p. 97–110
12. Matthews J, Zacharewski T. Differential binding affinities of PCBs, HO-PCBs, and aroclors with recombinant human, rainbow trout (Onchorhynkiss mykiss), and green anole (Anolis carolinensis) estrogen receptors, using a semi-high throughput competitive binding assay. Toxicol Sci 2000;53:326–339.
13. Moore M, Mustain M, Daniel K, Chen I, Safe S, Zacharewski T, Gillesby B, Joyeux A, Balaguer P. Antiestrogenic activity of hydroxylated polychlorinated biphenyl congeners identified in human serum. Toxicol Appl Pharmacol 1997;142:160–168.
14. Korach KS, Sarver P, Chae K, McLachlan JA, McKinney JD. Estrogen receptor-binding activity of polychlorinated hydroxybiphenyls—conformationally restricted structural probes. Mol Pharmacol 1988;33:120–126.
15. Connor K, Ramamoorthy K, Moore M, Mustain M, Chen I, Safe S, Zacharewski T, Gillesby B, Joyeux A, Balaguer P. Hydroxylated polychlorinated biphenyls (PCBs) as estrogens and antiestrogens: structure-activity relationships. Toxicol Appl Pharmacol 1997;145:111–123.
16. Brzozowski AM, Pike ACW, Dauter Z, Hubbard RE, Bonn T, Engstrom O, Ohman L, Greene GL, Gustafsson JA, Carlquist M. Molecular basis of agonism and antagonism in the oestrogen receptor. Nature 1997;389:753–758.
17. Pike ACW, Brzozowski AM, Hubbard RE, Bonn T, Thorsell AG, Engstrom O, Ljunggren J, Gustafsson JK, Carlquist M. Structure of the ligand-binding domain of oestrogen receptor beta in the presence of a partial agonist and a full antagonist. Embo J 1999;18:4608–4618.
18. Shiau AK, Barstad D, Loria PM, Cheng L, Kushner PJ, Agard DA, Greene GL. The structural basis of estrogen receptor/coactivator recognition and the antagonism of this interaction by tamoxifen. Cell 1998;95:927–937.
19. Anstead GM, Carlson KE, Katzenellenbogen JA. The estradiol pharmacophore: ligand structure-estrogen receptor binding affinity relationships and a model for the receptor binding site. Steroids 1997;62:268–303.
20. Beveridge DL, DiCapua FM. Free-energy via molecular simulation—applications to chemical and biomolecular systems. Annu Rev Biophys Biophys Chem 1989;18:431–492.
21. Mark AE. Free energy perturbation (FEP). In: von Ragné Schleyer, ed. Encyclopedia of Computational Chemistry. New York: John Wiley & Sons; 1998. p 1070–1083
22. Kollman P. Free-energy calculations—applications to chemical and biochemical phenomena. Chem Rev 1993;93:2395–2417.
23. Schäfer H, van Gunsteren WF, Mark AE. Estimating relative free energies from a single ensemble: hydration free energies. J Comput Chem 1999;20:1604–1617.
24. Mark AE, Xu YW, Liu HY, van Gunsteren WF. Rapid nonempirical approaches for estimating relative binding free energies. Acta Biochim Pol 1995;42:525–535.
25. Oostenbrink BC, Pitera JW, Van Lipzig MMH, Meerman JHN, van Gunsteren WF. Simulations of the estrogen receptor ligand-binding domain: affinity of natural ligands and xenoestrogens. J Med Chem 2000;43:4594–4605.
26. Pitera JW, van Gunsteren WF. One-step perturbation methods for solvation free energies of polar solutes. J Phys Chem B 2001;105:11264–11274.
27. Beutler TC, Mark AE, Van Schaik RC, Gerber PR, van Gunsteren WF. Avoiding singularities and numerical instabilities in free-energy calculations based on molecular simulations. Chem Phys Lett 1994;222:529–539.
28. Huo SH, Wang JM, Cieplak P, Kollman PA, Kuntz ID. Molecular dynamics and free energy analyses of cathepsin D-inhibitor interactions: insight into structure-based ligand design. J Med Chem 2002;45:1412–1419.
29. Wang JM, Morin P, Wang W, Kollman PA. Use of MM-PBSA in reproducing the binding free energies to HIV-1 RT of TIBO derivatives and predicting the binding mode to HIV-1 RT of efavirenz by docking and MM-PBSA. J Am Chem Soc 2001;123:5221–5230.
30. Aqvist J, Medina C, Samuelsson JE. New method for predicting

binding-affinity in computer-aided drug Design. Protein Eng 1994;7:385–391.
31. Aqvist J, Luzhkov VB, Brandsdal BO. Ligand binding affinities from MD simulations. Accounts Chem Res 2002;35:358–365.
32. Hansson T, Marelius J, Aqvist J. Ligand binding affinity prediction by linear interaction energy methods. J Comput-Aided Mol Des 1998;12:27–35.
33. Ljungberg KB, Marelius J, Musil D, Svensson P, Norden B, Aqvist J. Computational modelling of inhibitor binding to human thrombin. Eur J Pharm Sci 2001;12:441–446.
34. Scott WRP, Hünenberger PH, Tironi IG, Mark AE, Billeter SR, Fennen J, Torda AE, Huber P, Krüger P, van Gunsteren WF. The GROMOS biomolecular simulation program package. J Phys Chem A 1999;103:3596 – 3607.
35. van Gunsteren WF, Billeter SR, Eising AA, Hünenberger PH, Krüger P, Mark AE, Scott WRP, Tironi IG. Biomolecular simulation: The GROMOS96 manual and user guide. Zürich: Vdf Hochschulverlag AG an der ETH Zürich; 1996.
36. Berendsen HJC, Postma JPM, van Gunsteren WF, Hermans J. Interaction models for water in relation to protein hydration. In: Pullman BE, editor. Intermolecular forces. Dordrecht, The Netherlands: Reidel; 1981. p 331–342.
37. Berendsen HJC, Postma JPM, Van Gunsteren WF, Dinola A, Haak JR. Molecular-dynamics with coupling to an external bath. J Chem Phys 1984;81:3684–3690.
38. Ryckaert JP, Ciccotti G, Berendsen HJC. Numerical-integration of Cartesian equations of motion of a system with constraints—molecular-dynamics of N-alkanes. J Comput Phys 1977;23:327–341.
39. Tironi IG, Sperb R, Smith PE, van Gunsteren WF. A generalized reaction field method for molecular-dynamics simulations. J Chem Phys 1995;102:5451–5459.
40. Smith PE, van Gunsteren WF. Consistent dielectric properties of the simple point charge and extended simple point charge water models at 277 and 300 K. J Chem Phys 1994;100:3169–3174.
41. Bradbury SP, Mekenyan OG, Ankley GT. Quantitative structure-activity relationships for polychlorinated hydroxybiphenyl estrogen receptor binding affinity: an assessment of conformer flexibility. Environ Toxicol Chem 1996;15:1945–1954.
42. Vakharia DD, Gierthy JF. Use of a combined human liver microsome-estrogen receptor binding assay to assess potential estrogen modulating activity of PCB metabolites. Toxicol Lett 2000;114:55–65.
43. Kramer VJ, Helferich WG, Bergman A, KlassonWehler E, Giesy JP. Hydroxylated polychlorinated biphenyl metabolites are anti-estrogenic in a stably transfected human breast adenocarcinoma (MCF7) cell line. Toxicol Appl Pharmacol 1997;144:363–376.